JOURNAL OF COMPUTATIONAL PHYSICS 121, 281–297 (1995)

A Finite Element Formulation of the Darwin PIC Model for Use on Unstructured Grids

ERIC SONNENDRÜCKER

CEA Centre d'Etudes de Limeil-Valenton, Villeneuve-St-Georges, F-94195, France

AND

JOHN J. AMBROSIANO AND SCOTT T. BRANDON

Lawrence Livermore National Laboratory, Livermore, California

Received July 18, 1994; revised February 7, 1995

In this paper we introduce a new formulation of the Darwin approximation of Maxwell's equations and discuss its domain of applicability. We describe our finite element implementation of this model, allowing the use of unstructured grids, and its coupling with a PIC method for the particles. © 1995 Academic Press, Inc.

1. INTRODUCTION

Plasma behavior spans an enormous range of time and spatial scales. This is one reason why plasma are so challenging to model numerically. Collisionless plasma are fully described by the Vlasov–Maxwell system of equations:

$$\frac{\partial f}{\partial t} + \mathbf{v}\cdot\nabla_x f + \frac{q}{m}(\mathbf{E} + \mathbf{v}\times\mathbf{B})\cdot\nabla_v f = 0$$

$$-\frac{1}{c^2}\frac{\partial \mathbf{E}}{\partial t} + \nabla\times\mathbf{B} = \mu_0\mathbf{J}$$

$$\frac{\partial \mathbf{B}}{\partial t} + \nabla\times\mathbf{E} = 0$$

$$\nabla\cdot\mathbf{E} = \frac{\rho}{\varepsilon_0}$$

$$\nabla\cdot\mathbf{B} = 0.$$

The Maxwell equations describe the generation and propagation of electromagnetic waves, while the Vlasov equation governs the evolution of charged particle distributions in the multi-dimensional particle phase space. These equations are coupled by defining the current and charge density as moments of the particle distributions.

The Vlasov–Maxwell system can be directly simulated in a natural way by coupling the numerical integration of charged particle orbits at each time step to the advance of the electromagnetic fields on a grid of points. By now this technique, called particle-in-cell simulation (PIC) is very mature, and several good texts exist describing many variations on the theme in great detail [2, 7].

Nevertheless, there still remain many situations in which plasma modeling is extremely difficult. One of these occurs when the overall time scale of interest is very long compared with fundamental time scales of the plasma. The time scales most difficult to resolve over extended periods are the electron plasma oscillation period, the transit time of light waves over short distances, and often, in high-current regimes, the electron gyro-period.

Methods for dealing with temporal stiffness fall into two general categories: (1) implicit time differencing, which is equivalent to numerical time filtering, and (2) reduced physics models in which the governing equations are modified to eliminate the unwanted frequencies. Examples of the second approach go back to the very origins of plasma simulation in which models were almost exclusively electrostatic with no magnetic effects whatsoever.

An intriguing reduced physics model—the Darwin particle-in-cell formulation—was introduced by Nielson and Lewis in 1976 [17]. This model, as described in detail in the next section, eliminates only the propagating light waves from the system, while retaining other slower time scale electromagnetic effects arising from the particle current sources. It has proved to be a mixed blessing over the years. Many authors have used the technique to great advantage, but have noted the difficulties sometimes encountered in its implementation [3, 12, 17]. These problems arise from modifications of the originally hyperbolic system of equations which make the resulting system elliptic. Thus boundary conditions must be carefully formulated in order to ensure the problem is well-posed. Some of the most violent numerical instabilities experienced in plasma computations are

0021-9991/95 $12.00

associated with the naive implementation of the Darwin method. Recent interest has been shown in getting to the root of these problems. Several authors have written on the essential mathematical properties of the Darwin formulation [8, 18, 21]. There have also been significant advances in the efficiency of solving the Darwin field equations. Originally requiring many elliptic field solutions and numerous corrections, the technique has been recently streamlined to its bare essentials, realizing great savings in computation [4, 11].

An alternative to the Darwin formulation is time-implicit electromagnetics. Implicit electromagnetic simulations have successfully yielded good results in many applications. However, the properties of implicit methods are more difficult to assess than for a reduced model such as the Darwin approximation. In the Darwin model, the properties of the modified equations are relatively insensitive to the time step, provided the particle orbits and certain length scales are well resolved by the grid. On the other hand, implicit simulations filter all modes to some degree—the effect of the filter being sensitive to the relation between the time step and the particular frequency being sampled. Therefore in some regimes, the Darwin method may be "cleaner" to analyze and interpret.

Besides the stiffness problems encountered in plasma simulation, there is another aspect that has become an increasing challenge as interest in plasma technology applications has grown. Real plasma devices seldom fit the orderly regular grids on which plasma simulations were originally implemented years ago. A number of investigators have published promising new techniques transcribing plasma computations to more flexible meshes. These include curvilinear, but otherwise regular meshes [13, 19], as well as completely unstructured meshes [14, 1, 5, 15]. The techniques employed have included finite differences (in curvilinear coordinates) [13, 19], finite volumes [5, 15], and finite elements [14, 1]. These have so far been applied in fully electromagnetic as well as reduced physics models.

In this paper we will bring together several advances to produce a state-of-the-art formulation of the Darwin model. Building on recent analyses of the Darwin system of equations, we will introduce a comprehensive statement of boundary conditions under which the problem may be considered well-posed. Using dispersion analysis we will examine the fundamental stability criteria for Darwin simulations. We will show precisely how the full electromagnetic dispersion relation is modified in the reduced model. A constrained, mixed variational, finite element formulation will be described which solves the Darwin field problem in the electric and magnetic field components on an unstructured finite element mesh. This permits the method to be used in virtually any geometry. Test problems will be presented which demonstrate the accuracy of the new formulation when compared against analytical benchmarks. Although described in two dimensions, the method is fully three dimensional.

2. THE DARWIN MODEL

The Darwin approximation of Maxwell's equations is introduced to remove what is often the stiffest time scale in electromagnetic simulations, namely the propagation time of light waves from zone to zone. This model eliminates electromagnetic waves, but keeps an important part of the physics, in particular the low frequency phenomena.

The electric field $\mathbf{E}$ is decomposed into two parts, an irrotational part $\mathbf{E}_{\text{irr}}$ which is curl free and a solenoidal part $\mathbf{E}_{\text{sol}}$ which is divergence free:

$$\mathbf{E} = \mathbf{E}_{\text{irr}} + \mathbf{E}_{\text{sol}}$$

where

$$\nabla \times \mathbf{E}_{\text{irr}} = 0, \quad \nabla \cdot \mathbf{E}_{\text{sol}} = 0.$$

Furthermore, as $\nabla \times \mathbf{E}_{\text{irr}} = 0$ we can write $\mathbf{E}_{\text{irr}} = -\nabla\phi$.

Darwin's approximation consists in dropping the solenoidal part of the displacement current from Ampere's law:

$$\nabla \times \mathbf{B} = \mu_0 \mathbf{J} + \frac{1}{c^2}\frac{\partial \mathbf{E}_{\text{irr}}}{\partial t} + \frac{1}{c^2}\frac{\partial \mathbf{E}_{\text{sol}}}{\partial t}.$$

Taking the curl of this equation, we obtain

$$\nabla \times \nabla \times \mathbf{B} = \mu_0 \nabla \times \mathbf{J}$$

which is an elliptic equation for $\mathbf{B}$.

By dropping only the solenoidal part of the displacement current, charge conservation remains satisfied in the Darwin model.

Taking the curl of Faraday's law yields an elliptic equation for $\mathbf{E}_{\text{sol}}$,

$$\nabla \times \nabla \times \mathbf{E} = -\frac{\partial}{\partial t} \nabla \times \mathbf{B}.$$

Lastly, $\nabla \cdot \mathbf{E} = \rho/\varepsilon_0$ gives us Poisson's equation for the electrostatic potential,

$$-\nabla^2 \phi = \frac{\rho}{\varepsilon_0}.$$

Instead of Maxwell's equations, which are hyperbolic, we now have three elliptic equations. Thus the Courant condition on stability no longer constrains the time step. In addition to imposing appropriate boundary conditions, we must also ensure that any solution will be consistent with the constraints $\nabla \cdot \mathbf{E}_{\text{sol}} = 0$ and $\nabla \cdot \mathbf{B} = 0$.

2.1. *Applicability of the Darwin Model*

Many who have encountered the Darwin formulation have found it awkward to pin down the regime in which it is clearly advantageous over fully electromagnetic models, on the one hand, and over static descriptions (electrostatic or magnetostatic), on the other. In an attempt to clarify the discussion, consider the following scaling argument:

Confronted with a plasma physics problem, involving a device of length L, where we are mostly interested in low frequency phenomena (typically phenomena involving ions) we scale Maxwell's equation in the following way:

Let L be the characteristic length of the problem, τ its characteristic time, e.g., the frequency in which we are interested.

We then obtain the dimensionless form of Maxwell's equations,

$$-\varepsilon \frac{\partial \mathbf{E}}{\partial t} + \nabla \times \mathbf{B} = \mathbf{J}$$

$$\varepsilon \frac{\partial \mathbf{B}}{\partial t} + \nabla \times \mathbf{E} = 0,$$

where $\varepsilon = L/\tau c$.

We can now Taylor expand $\mathbf{E}$ and $\mathbf{B}$ with respect to ε:

$$\mathbf{E} = \mathbf{E}_0 + \varepsilon \mathbf{E}_1 + \cdots$$

$$\mathbf{B} = \mathbf{B}_0 + \varepsilon \mathbf{B}_1 + \cdots.$$

It has been shown in special cases [8, 18] that the quasistatic approximation (time derivatives neglected) agrees with Maxwell's equations up to first order; i.e., $\mathbf{E}_0$ and $\mathbf{B}_0$ are the same but $\mathbf{E}_1$ and $\mathbf{B}_1$ differ. And the Darwin model coincides with Maxwell's equations up to second order. This result can be extended to the general 3D case.

Thus, for small ε these approximations are justified. Moreover, in some situations, especially in magnetized plasma, it is essential to keep the first-order term, which will support electromagnetic phenomena. These include Alfven waves, ion micro-instabilities, and others. As shown in Appendix A, modeling low frequency phenomena in a strongly magnetized plasma is a good fit to the Darwin model.

Indeed, there is a particular regime in which the Darwin model fits well. Moreover, this regime is broadened considerably when further approximations are introduced to reduce the problem such as the use of fluid electrons.

2.2. *Boundary Conditions*

For some problems, as in our benchmark test which assumes periodicity, the boundary conditions are not an issue. In this case, provided the different quantities average to zero, the problem is well-posed.

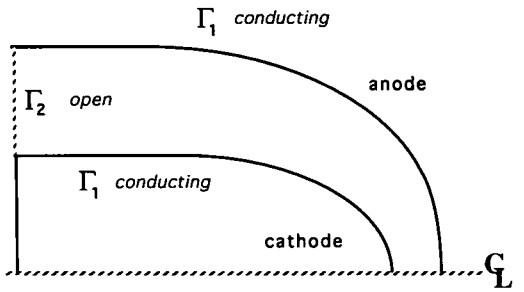

FIG. 1. A hypothetical diode device with both open and conducting boundaries. The anode and cathode surfaces (Γ_1) are conducting while the waveguide inlet (Γ_2) is open. The bottom boundary is simply a symmetry boundary representing the centerline of the axisymmetric diode.

For bounded problems, in general, one must introduce an additional, nonphysical, boundary condition on $\mathbf{E}_{irr}$ or $\mathbf{E}_{sol}$ to ensure that the decomposition of $\mathbf{E}$ is unique.

Note that a vector field $\mathbf{E}$ of the form ∇u, where $\nabla^2 u = 0$, satisfies both $\nabla \cdot \mathbf{E} = 0$ and $\nabla \times \mathbf{E} = 0$. Therefore the field can be regarded as either irrotational or solenoidal. The extra boundary condition is needed to uniquely categorize such a field.

There are many different possibilities for these boundary conditions. A guideline for picking boundary conditions that is consistent with the asymptotics of the Darwin approximation is found in Degond and Raviart [8]. Applied strictly to conducting boundaries, the method takes account of the v/c scaling of Maxwell's equations. Boundary conditions for the Darwin approximation are chosen so as to retain second-order accuracy in v/c. An alternative formulation, based on physical considerations related to surface charge, was also proposed by Weitzner and Lawson [21].

To make the discussion more concrete, consider the following example. Suppose we wish to model a device which is conducting on some subset of the boundary (Γ_1) and "open" on (Γ_2) as shown in Fig. 1.

Appropriate boundary conditions for a fully electromagnetic simulation would be:

$$\mathbf{E} \times \mathbf{n} = 0 \quad \text{on } \Gamma_1 \tag{2.1}$$

$$(\mathbf{E} - c\mathbf{B} \times \mathbf{n}) \times \mathbf{n} = 0 \quad \text{on } \Gamma_2. \tag{2.2}$$

The first condition simply states that an electric field tangent to the surface of the conductor cannot exist. The second is a free-wave boundary condition also called the "Silver–Müller" condition.

Using Maxwell's equations, we can decouple the Silver–Müller boundary condition into conditions on the $\mathbf{E}$ and $\mathbf{B}$ fields, respectively:

$$\frac{1}{c}\frac{\partial \mathbf{E}}{\partial t} \times \mathbf{n} \times \mathbf{n} = (\nabla \times \mathbf{E}) \times \mathbf{n} \tag{2.3}$$

$$\frac{1}{c}\frac{\partial \mathbf{B}}{\partial t} \times \mathbf{n} \times \mathbf{n} = (\nabla \times \mathbf{B}) \times \mathbf{n} - \mu_0 \mathbf{J} \times \mathbf{n}. \tag{2.4}$$

Moreover, $\mathbf{E} \times \mathbf{n} = 0$ on Γ_1 implies, using Faraday's law, that

$$\frac{\partial}{\partial t}\mathbf{B} \cdot \mathbf{n} = 0 \quad \text{on } \Gamma_1; \quad \frac{\partial}{\partial t}\int_{\Gamma_{2i}} \mathbf{B} \cdot \mathbf{n}\, d\sigma = 0$$

and, also, using Ampere's law,

$$(\nabla \times \mathbf{B}) \times \mathbf{n} = \mu_0 \mathbf{J} \times \mathbf{n} \quad \text{on } \Gamma_1.$$

In the Darwin limit, we must have appropriate boundary conditions for each of the component fields $\mathbf{E}_{\text{sol}}$ and $\mathbf{E}_{\text{irr}}$, even though this decomposition is completely artificial. Motivated in part by physical considerations and in part by the analysis of Degond and Raviart, we choose

$$\mathbf{E}_{\text{irr}} \times \mathbf{n} = 0 \quad \text{on } \Gamma_1$$

$$\int_{\Gamma_{1i}} \mathbf{E}_{\text{sol}} \cdot \mathbf{n}\, d\sigma = 0$$

$$\mathbf{E}_{\text{sol}} \cdot \mathbf{n} = 0 \quad \text{on } \Gamma_2,$$

where Γ_{1i} (Γ_{2i}), $i = 1, \ldots, n$, are piecewise smooth components of Γ_1 (Γ_2). These boundary conditions state that on conducting boundaries, the electric field will be normal to the surface and driven by $\mathbf{E}_{\text{sol}}$, while on open boundaries, electric fields will be tangential and driven by $\mathbf{E}_{\text{irr}}$. With the above conditions we can close the system of equations which becomes:

For the scalar potential

$$-\nabla^2 \phi = \frac{\rho}{\varepsilon_0} \tag{2.5}$$

$$\phi = V_i \quad \text{on } \Gamma_{1i} \tag{2.6}$$

$$\frac{\partial \phi}{\partial n} = g \quad \text{on } \Gamma_2. \tag{2.7}$$

The magnetic field satisfies, supposing that $\mathbf{B}_0 = 0$,

$$\nabla \times \nabla \times \mathbf{B} = \mu_0 \nabla \times \mathbf{J} \tag{2.8}$$

$$\nabla \cdot \mathbf{B} = 0 \tag{2.9}$$

$$(\nabla \times \mathbf{B}) \times \mathbf{n} = \mu_0 \mathbf{J} \times \mathbf{n} \quad \text{on } \Gamma_1 \tag{2.10}$$

$$\mathbf{B} \cdot \mathbf{n} = 0 \quad \text{on } \Gamma_1 \tag{2.11}$$

$$(\nabla \times \mathbf{B}) \times \mathbf{n} = \mu_0 \mathbf{J} \times \mathbf{n} + \frac{1}{c}\frac{\partial \mathbf{B}}{\partial t} \times \mathbf{n} \times \mathbf{n} \quad \text{on } \Gamma_2 \tag{2.12}$$

$$\int_{\Gamma_{2i}} \mathbf{B} \cdot \mathbf{n}\, d\sigma = 0 \tag{2.13}$$

while the solenoidal electric field is obtained from

$$\nabla \times \nabla \times \mathbf{E}_{\text{sol}} - \frac{1}{c^2}\nabla \ddot{\phi} = -\mu_0 \dot{\mathbf{J}} \tag{2.14}$$

$$\nabla \cdot \mathbf{E}_{\text{sol}} = 0 \tag{2.15}$$

$$\mathbf{E}_{\text{sol}} \times \mathbf{n} = 0 \quad \text{on } \Gamma_1 \tag{2.16}$$

$$\int_{\Gamma_{1i}} \mathbf{E}_{\text{sol}} \cdot \mathbf{n}\, d\sigma = 0 \tag{2.17}$$

$$\ddot{\phi} = \ddot{V}_i \quad \text{on } \Gamma_{1i} \tag{2.18}$$

$$(\nabla \times \mathbf{E}_{\text{sol}}) \times \mathbf{n} = \frac{1}{c}\frac{\partial \mathbf{E}_{\text{irr}}}{\partial t} \times \mathbf{n} \times \mathbf{n} \quad \text{on } \Gamma_2 \tag{2.19}$$

$$\mathbf{E}_{\text{sol}} \cdot \mathbf{n} = 0 \quad \text{on } \Gamma_2. \tag{2.20}$$

Note that to obtain (2.19), we have neglected the solenoidal part of the displacement current with respect to the irrotational part in (2.3). This is completely consistent with the approximation to Ampere's law in the Darwin limit. It is interesting that condition (2.2), which is a statement about the fate of normally incident electromagnetic waves in the full set of Maxwell's equations, can still be applied in the Darwin limit in which no electromagnetic waves propagate. Nevertheless, this is a perfectly consistent way of obtaining open boundary conditions on the fields and, as we shall see, it works quite well.

3. VARIATIONAL FORMULATION

We now turn to the variational formulation of the model. This not only enables us to demonstrate that each system is well-posed, it also provides the essential framework for a finite element discretization.

3.1. *Poisson's Equation*

For the convenience of readers unfamiliar with variational formulations or finite elements, we shall carefully derive a variational formulation from system (2.5)–(2.7). The variational form of Poisson's equation involves the straightforward application of the standard technique. Let ψ be a smooth test function. Multiplying Eq. (2.5) by ψ and integrating over Ω yields

$$-\int_\Omega \nabla^2 \phi \psi\, d\mathbf{x} = \int_\Omega \frac{\rho}{\varepsilon_0}\psi\, d\mathbf{x};$$

then, using Green's theorem,

$$-\int_\Omega \nabla^2\phi\psi\,d\mathbf{x} = \int_\Omega \nabla\phi\cdot\nabla\psi\,d\mathbf{x} - \int_\Gamma \frac{\partial\phi}{\partial n}\psi\,d\sigma, \quad (3.1)$$

we obtain

$$\int_\Omega \nabla\phi\cdot\nabla\psi\,d\mathbf{x} - \int_\Gamma \frac{\partial\phi}{\partial n}\psi\,d\sigma = \frac{1}{\varepsilon_0}\int_\Omega \rho\psi\,d\mathbf{x}. \quad (3.2)$$

Boundary conditions are dealt with in two different ways:

• (2.6) is called an essential boundary condition. For such boundary conditions the problem is brought back to vanishing boundary conditions by setting $\tilde{\phi} = \phi - \beta$, where β is any function satisfying (2.6). Then we look for $\tilde{\phi}$ in a function space where all functions vanish on Γ_1. Practically, this means that the test functions have to vanish on this part of the boundary, which is enough to get a solution with the same property.

• (2.7) is called a natural boundary condition. In (3.2) we simply need to replace $\partial\phi/\partial n$ by its known value on the boundary to enforce boundary condition (2.7).

Our data being time dependent, the variational formulation for our Poisson system at time t is then stated as

Find $\tilde{\phi}(t) \in H_1(\Omega)$ *such that*

$$\int_\Omega \nabla\tilde{\phi}\cdot\nabla\psi\,d\mathbf{x} = \frac{1}{\varepsilon_0}\int_\Omega \rho\psi\,d\mathbf{x} + \int_{\Gamma_2} g\psi\,d\sigma - \int_\Omega \nabla\beta\cdot\nabla\psi\,d\mathbf{x} \quad \forall\psi\in H_1(\Omega), \quad (3.3)$$

where $H_1(\Omega) = \{\psi \in H^1(\Omega);\ \psi = 0 \text{ on } \Gamma_1\}$.

Then, knowing $\tilde{\phi}$, we have $\phi = \tilde{\phi} + \beta$. We remind the reader that $\psi \in H^1(\Omega)$ simply means that ψ, as well as all its spatial derivatives, are square integrable.

3.2. *The Constrained Problems*

The remaining systems are more difficult to formulate as they represent systems of vector and scalar fields with imposed constraints. This area has been intensively studied in recent years, particularly with regard to incompressible hydrodynamic flow. Mixed variational formulations, i.e., those in which different quantities live in different, but compatible, Sobolev spaces, have been used extensively, for example, by Girault and Raviart [10]. More recently Assous *et al.* [1] have used Lagrange multipliers with a mixed finite element technique to enforce charge conservation in a fully electromagnetic formulation.

In the present context, we must enforce the $\nabla\cdot\mathbf{B} = 0$ constraint in the solution for $\mathbf{B}$. This is done by explicitly adding a Lagrange multiplier p which has the trivial solution (i.e., vanishes) in the continuum limit, but which will play a vital role in absorbing numerical errors when discretized. Some authors also call this approach a penalty method.

Thus with the addition of the Lagrange multiplier, (2.8) becomes

$$\nabla\times\nabla\times\mathbf{B} - \nabla p = \mu_0\nabla\times\mathbf{J}. \quad (3.4)$$

Now let $\mathbf{C}$ be a smooth function and take the dot product of (3.4) with $\mathbf{C}$:

$$\int_\Omega \nabla\times\nabla\times\mathbf{B}\cdot\mathbf{C}\,d\mathbf{x} - \int_\Omega \nabla p\cdot\mathbf{C}\,d\mathbf{x} = \mu_0\int_\Omega \nabla\times\mathbf{J}\cdot\mathbf{C}\,d\mathbf{x}. \quad (3.5)$$

Using a Green formula we get

$$\int_\Omega \nabla\times\nabla\times\mathbf{B}\cdot\mathbf{C}\,d\mathbf{x} = \int_\Omega (\nabla\times\mathbf{B})\cdot(\nabla\times\mathbf{C})\,d\mathbf{x} - \int_\Gamma ((\nabla\times\mathbf{B})\times\mathbf{n})\cdot\mathbf{C}\,d\sigma.$$

Replacing the boundary term using (2.10) and (2.12) yields

$$\int_\Omega \nabla\times\nabla\times\mathbf{B}\cdot\mathbf{C}\,d\mathbf{x} = \int_\Omega (\nabla\times\mathbf{B})\cdot(\nabla\times\mathbf{C})\,d\mathbf{x} - \mu_0\int_\Gamma (\mathbf{J}\times\mathbf{n})\cdot\mathbf{C}\,d\sigma - \frac{1}{c}\int_{\Gamma_2}\frac{\partial}{\partial t}\mathbf{B}\times\mathbf{n}\times\mathbf{n}\cdot\mathbf{C}. \quad (3.6)$$

We can transform the right-hand side using again Green's formula:

$$\int_\Omega (\nabla\times\mathbf{J})\cdot\mathbf{C}\,d\mathbf{x} = \int_\Omega \mathbf{J}\cdot(\nabla\times\mathbf{C})\,d\mathbf{x} - \int_\Gamma \mathbf{J}\times\mathbf{n}\cdot\mathbf{C}\,d\sigma. \quad (3.7)$$

The remaining term in (3.5) is transformed using another Green's formula:

$$\int_\Omega \nabla p\cdot\mathbf{C}\,d\mathbf{x} = -\int_\Omega p\nabla\cdot\mathbf{C}\,d\mathbf{x} + \int_\Gamma p\mathbf{C}\cdot\mathbf{n}\,d\sigma. \quad (3.8)$$

For the boundary term we will impose $\mathbf{C}\cdot\mathbf{n} = 0$ on Γ_1 which will lead to (2.11) and we also assume that $p = 0$ on Γ_2.

Now, replacing all the terms in (3.5) using (3.6), (3.7), and (3.8) yields

$$\int_\Omega (\nabla \times \mathbf{B}) \cdot (\nabla \times \mathbf{C})\, d\mathbf{x} + \int_\Omega p \nabla \cdot \mathbf{C}\, d\mathbf{x} + \frac{d}{dt} \int_{\Gamma_2} (\mathbf{B} \times \mathbf{n}) \cdot (\mathbf{C} \times \mathbf{n})\, d\sigma = \mu_0 \int_\Omega \mathbf{J} \cdot (\nabla \times \mathbf{C})\, d\mathbf{x}. \tag{3.9}$$

Multiplying (2.9) by a scalar test function q yields

$$\int_\Omega (\nabla \cdot \mathbf{B}) q\, d\mathbf{x} = 0. \tag{3.10}$$

In order to handle the essential boundary conditions, we shall look for a solution in the space

$$H_2(\Omega) = \left\{ \mathbf{C} \in H(\text{curl}, \Omega) \cap H(\text{div}, \Omega);\ \mathbf{C} \times \mathbf{n} \in L^2(\Gamma_2),\ \mathbf{C} \cdot \mathbf{n} = 0 \quad \text{on } \Gamma_1,\ \int_{\Gamma_{2i}} \mathbf{C} \cdot \mathbf{n}\, d\sigma = 0 \right\}.$$

One additional modification is needed to accommodate the numerical method which is described in detail below. We require the matrix associated to $\mathbf{B}$ in (3.9) to be invertible, which is not the case as (3.9) stands, for the kernel of the bilinear form $\int_\Omega \nabla \times \mathbf{B} \cdot \nabla \times \mathbf{C}\, d\mathbf{x}$ contains all the gradients and thus is not reduced to 0. However, since (3.10) implies that $\nabla \cdot \mathbf{B} = 0$, we may simply add the term $\int_\Omega \nabla \cdot \mathbf{B} \nabla \cdot \mathbf{C}\, d\mathbf{x}$ to the left-hand side of (3.9), which will give us a bilinear form with a vanishing kernel on $H_2(\Omega)$ and thus numerically an invertible matrix. This done, we finally obtain the variational statement for $\mathbf{B}$:

Find $(\mathbf{B}(t), p(t)) \in H_2(\Omega) \times L^2(\Omega)$ *such that*

$$\int_\Omega (\nabla \times \mathbf{B}) \cdot (\nabla \times \mathbf{C})\, d\mathbf{x} + \int_\Omega \nabla \cdot \mathbf{B} \nabla \cdot \mathbf{C}\, d\mathbf{x} + \frac{1}{c} \frac{d}{dt} \int_{\Gamma_2} (\mathbf{B} \times \mathbf{n}) \cdot (\mathbf{C} \times \mathbf{n})\, d\sigma + \int_\Omega p \nabla \cdot \mathbf{C}\, d\mathbf{x} = \mu_0 \int_\Omega \mathbf{J} \cdot (\nabla \times \mathbf{C})\, d\mathbf{x} \quad \forall \mathbf{C} \in H_2(\Omega) \tag{3.11}$$

$$\int_\Omega (\nabla \cdot \mathbf{B}) q\, d\mathbf{x} = 0 \qquad \forall q \in L_2(\Omega). \tag{3.14}$$

As we mentioned earlier, it is easy to show from (3.11) that p vanishes in the continuum formulation.

Let ξ be the solution of

$$\nabla^2 \xi = p, \quad \frac{\partial \xi}{\partial n} = 0 \quad \text{on } \Gamma_1, \quad \xi = 0 \quad \text{on } \Gamma_2.$$

Now take $\mathbf{C} = \nabla \xi$. Then $\mathbf{C}$ satisfies

$$\nabla \times \mathbf{C} = 0, \quad \nabla \cdot \mathbf{C} = p, \quad \mathbf{C} \cdot \mathbf{n} = \frac{\partial \xi}{\partial n} = 0 \quad \text{on } \Gamma_1.$$

Hence $\mathbf{C}$ is in $H_2(\Omega)$. Furthermore, $\nabla \cdot \mathbf{B} = 0$ from (3.14). Since $\nabla \times \mathbf{C} = 0$, $\nabla \cdot \mathbf{C} = p$, and $\mathbf{C} \times \mathbf{n} = 0$ on Γ_2, (3.11) yields

$$\int_\Omega p^2\, d\mathbf{x} = 0$$

from which it follows that $p = 0$.

The system for $\mathbf{E}_{\text{sol}}$ is completely analogous to the system for $\mathbf{B}$. We therefore simply write down the variational form without rederiving it here:

Find $(\mathbf{E}_{\text{sol}}(t), \ddot{\phi}(t)) \in H_3(\Omega) \times M(\Omega)$ *such that*

$$\int_\Omega (\nabla \times \mathbf{E}_{\text{sol}}) \cdot (\nabla \times \mathbf{F})\, d\mathbf{x} + \int_\Omega \nabla \cdot \mathbf{E}_{\text{sol}} \nabla \cdot \mathbf{F}\, d\mathbf{x} + \frac{1}{c^2} \int_\Omega \ddot{\phi} \nabla \cdot \mathbf{F}\, d\mathbf{x} = -\mu_0 \int_\Omega \dot{\mathbf{J}} \cdot \mathbf{F}\, d\mathbf{x} + \frac{1}{c^2} \int_\Omega \ddot{V} \mathbf{F} \cdot \mathbf{n}\, d\sigma - \frac{1}{c} \frac{d}{dt} \int_{\Gamma_2} (\mathbf{E}_{\text{irr}} \times \mathbf{n}) \cdot (\mathbf{F} \times \mathbf{n})\, d\sigma \quad \forall \mathbf{F} \in H_3(\Omega) \tag{3.13}$$

$$\int_\Omega (\nabla \cdot \mathbf{E}_{\text{sol}})\, \psi\, d\mathbf{x} = 0 \quad \forall \psi \in M(\Omega), \tag{3.14}$$

where $H_3(\Omega) = \{\mathbf{F} \in H(\Omega, \text{curl}) \cap H(\Omega, \text{div}) : \mathbf{F} \times \mathbf{n} = 0 \text{ on } \Gamma_1,\ \mathbf{F} \cdot \mathbf{n} = 0 \text{ on } \Gamma_2,\ \int_{\Gamma_{1,i}} \mathbf{F} \cdot \mathbf{n}\, d\sigma = 0\}$ and $M(\Omega) = \{\zeta \in L^2(\Omega) : \int_\Omega \zeta \chi_i\, d\mathbf{x} = 0,\ i = 1, \ldots, n\}$.

The set $\{\chi_i\}_{i=1,\ldots,n}$ is defined by

$$\nabla^2 \chi_i = 0, \quad \chi_i = \delta_{ij} \quad \text{on } \Gamma_{1j}, \quad \frac{\partial \chi}{\partial n} = 0 \quad \text{on } \Gamma_2,$$

where n is the number of continuously connected smooth segments of Γ_1. The well-posedness of the problems (3.11)–(3.12) and (3.13)–(3.14) follows from the ellipticity of the bilinear forms in the chosen function spaces. The proof is based on classical inf–sup theory that can be found for example in Girault and Raviart [10].

4. SPATIAL DISCRETIZATION OF THE FIELD EQUATIONS

At each time step, we are required to solve two different kinds of problems: a traditional Poisson problem (3.3) and two constrained problems (3.11)–(3.12) and (3.13)–(3.14). The latter will require compatible finite element spaces to be well-

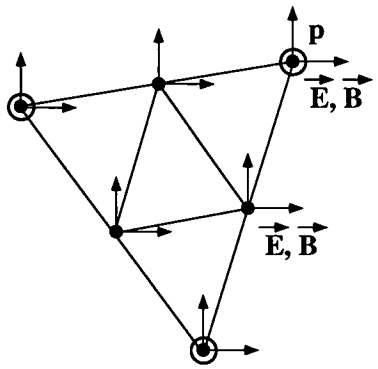

FIG. 2. The Taylor–Hood element. The electric and magnetic field vectors are defined at the vertices of each of the finer triangles, while the Lagrange multipliers are known only at the vertices of the coarser ones. The differences in the degrees of freedom are necessary to ensure compatibility of the respective function spaces.

posed and convergent. Such problems have been well studied in hydrodynamics and several possible finite elements are given in Girault and Raviart [10]. We must bear in mind that (3.3) is to be solved on the same grid. Therefore, following Assous *et al.* [1], we choose a modified version of the Taylor–Hood element (Fig. 2).

To build a suitable grid, a mesh generator first constructs a slightly coarser mesh of triangles than desired for resolving the vector fields. Then each triangle is subdivided into four smaller ones by joining the midpoints of each side to produce the degrees of freedom required for the Taylor–Hood elements. In the Taylor–Hood element the scalar quantities are traditionally linear on each element and so have three degrees of freedom which are the values at the vertices. The vector quantities are quadratic and thus have six degrees of freedom which are the values at the vertices and the midpoints. Several authors (e.g., Assous *et al.* [1]) have gotten good results with a simpler representation where the vectors are linear on the fine grid, leading to the same degrees of freedom.

To have the same resolution in $\mathbf{E}_{\text{irr}}$ as in $\mathbf{E}_{\text{sol}}$, Poisson's equation (3.3) will be solved on the finer grid, with linear shape functions on each of the small triangles. As for the mixed problems, the vector fields will be evaluated at the vertices of the small triangles assuming linear sub-elements while the Lagrange multipliers will be evaluated only at the vertices of the larger triangles treating them as linear elements as well. It follows that the solution will be less precise for the Lagrange multipliers, but this is not a concern, since they are only needed to enforce the constraints.

We introduce the following notation:

Let n_h be the number of vertices of the finer grid and n_{2h} be the number of vertices of the coarser grid. Let τ_h be the fine triangulation composed of triangles T_h and τ_{2h} be the coarse triangulation composed of triangles T_{2h}. And finally, let $\{a_i\}$, $i = 1, \ldots, n_h$, be the vertices of the small triangles.

To discretize (3.3), we introduce a finite dimensional subspace of $H^1(\Omega)$,

$$H_h = \{\phi_h \in C^0(\overline{\Omega});\ \forall T_h \in \tau_h,\ \phi_{h,K_h} \in P_1,\ \phi_h = 0 \text{ on } \Gamma_1\},$$

where P_1 is the set of polynomials of degree one.

For any $\phi \in H_h$ we have

$$\phi(x, t) = \sum_{i=1}^{n_h} \phi^i(t) N^i(x), \tag{4.1}$$

where $\{N^i\}_{i=1,\ldots,n_h;\, a_i \notin \Gamma_1}$ is a basis of H_h.

N_i is the function of H_h satisfying $N^i(a_i) = 1$ and $N^i(a_j) = 0$ for $i \neq j$. To enforce $N^i(x) = 0$ on Γ_1 we require that $N^i(a_i) = 0$ if $a_i \in \Gamma_1$.

The finite dimensional version of (3.3) now becomes

Find $\phi(t) \in H_h$ *such that*

$$\int_\Omega \nabla\phi_h \cdot \nabla\psi_h \, d\mathbf{x} = \frac{1}{\varepsilon_0}\int_\Omega \rho_h\psi_h \, d\mathbf{x} + \int_{\Gamma_2} g_h\psi_h \, d\sigma \quad \forall\psi_h \in H_h. \tag{4.2}$$

Using (4.1) for the different functions and replacing ψ_h by N_j for $1 \leq j \leq n_h$ we get

$$\sum_{i=1}^{n_h} \phi^i \int_\Omega \nabla N^i \cdot \nabla N^j \, d\mathbf{x} = \frac{1}{\varepsilon_0}\sum_{i=1}^{n_h} \rho^i \int_\Omega N^i \cdot N^j \, d\mathbf{x} + \sum_{i=1}^{n_h} g^i \int_{\Gamma_2} N^i \cdot N^j \, d\sigma. \tag{4.3}$$

Now let K be the $n_h \times n_h$ matrix whose i, j term is $\int_\Omega \nabla N^i \cdot \nabla N^j \, d\mathbf{x}$. Let M be the $n_h \times n_h$ matrix whose i, j term is $\int_\Omega N^i \cdot N^j \, d\mathbf{x}$, and let M^{Γ_2} be the $n_h \times n_h$ matrix whose i, j term is $\int_{\Gamma_2} N^i \cdot N^j \, d\sigma$.

Then, in matrix form, (4.3) can be written

$$K\phi_h = \frac{1}{\varepsilon_0} M\rho_h + M^{\Gamma_2} g_h. \tag{4.4}$$

Solving (4.4) for ϕ_h using a classical ICCG solver will give the values of the electrostatic potential at the vertices of the triangulation τ_h.

The finite element formulation of (3.11)–(3.12) and (3.13)–(3.14) can be derived in a similar way. A short description an the final formulations can be found in Appendix B. In matrix form, we get two linear systems of the same structure which is

$$Ku + L^t p = b$$

$$Lu = 0.$$

K is a square matrix of side $3n_h$ and L is a $n_h \times n_{2h}$ rectangular matrix and so is not invertible. Therefore the system is completely coupled.

Multiplying the first equation by LK^{-1} and using $Lu = 0$ yields

$$LK^{-1}L'p = LK^{-1}b \tag{4.5}$$

which is independent of u. To solve (4.5) we use a nested iteration technique. In particular, a gradient method is used to solve for p, with iterates of u and p being computed at each step. To solve for these, we use a conjugate gradient method on the linear system involving the matrix K. This combination is called the Uzawa method, and the full algorithm is described in [9].

At each step we need to solve a linear system involving the matrix K, which is done with another conjugate gradient. This could be very costly if the number of outer iterations were large. This is not the case for our problems. For $\mathbf{B}$ we only need the outer iterations to clean out divergence errors, which is generally done in at most a couple of iterations, and so this method competes fairly well with a traditional Poisson correction. And even for $\mathbf{E}_{\text{sol}}$, where we need to extract the divergence free part of a normally nonsolenoidal solution, we take advantage of the fact that $LK^{-1}L^T$ is a much smaller matrix than K and that we do not need high precision on p.

The scheme described above is fully applicable in three dimensions. In our present two-dimensional implementation we have built the code to accommodate either rectangular or axisymmetric coordinates.

5. COUPLING THE PARTICLES AND FIELDS

The following section describes the way in which particles are advanced and coupled with the field solutions.

5.1. *Particle Integration*

The Darwin model of a collisionless plasma couples the field equations to particle motion at each time step. Each macroparticle, represented by its position and momentum, obeys

$$\frac{d\mathbf{x}_k}{dt} = \mathbf{v}_k$$

$$\frac{d\mathbf{p}_k}{dt} = q_k(\mathbf{E} + \mathbf{v} \times \mathbf{B}),$$

where $\mathbf{p}_k = \gamma_k m_k \mathbf{v}_k$ and $\gamma_k = (1 + \mathbf{p}_k^2/m_k^2c^2)^{1/2}$.

Here we have chosen the full relativistic form of the Lorenz force equation for robustness.

Numerically, the equation of motion

$$\frac{d\gamma_k m_k \mathbf{v}_k}{dt} = q_k(\mathbf{E} + \mathbf{v}_k \times \mathbf{B})$$

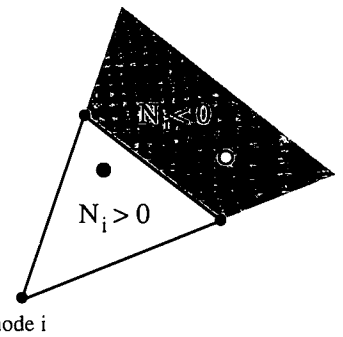

FIG. 3. The value of the linear element basis function for a given node is positive inside the element and becomes negative as one crosses the opposite triangle edge. This property can be used to judge whether a particle is inside or outside a particular element.

in integrated using a standard Boris push which is comprised of three steps: (1) an initial half acceleration from the electric field; (2) a rotation due to the magnetic field; and (3) a final half electric field acceleration.

The position is then advanced using

$$\frac{d\mathbf{x}_k}{dt} = \mathbf{v}_k.$$

One of the problems encountered when one abandons a regular, uniform grid for an irregular one is locating the particles. This is trivial on the regular mesh with its constant spacing, but not so on an unstructured mesh. To assign a particle to a particular element, in order to allocate its charge or current, requires a suitable algorithm for particle tracking. A method proposed in [14], makes use of the barycentric coordinates of a particle with respect to a triangle. These coordinates are closely related to the linear element basis functions for triangles.

Consider a triangle T_h. The barycentric coordinates of a particle with respect to a_1, a_2, a_3, the vertices of T_h, are the same as the linear element basis functions N_1, N_2, N_3 evaluated at the particle location (see Fig. 3); i.e.,

$$N_i(a_i) = 1, \quad N_i(a_j) = 0 \quad \text{for } i \neq j.$$

The values of these functions at the particle coordinates can help to determine its location relative to a given element. For example, if upon evaluating N_1 at particle position $\mathbf{x}_k$ we find $N_1(\mathbf{x}_k) > 0$, it means that a_1 and $\mathbf{x}_k$ are on the same side of the line (a_2a_3), whereas $N_1(\mathbf{x}_k) < 0$ means that a_1 and $\mathbf{x}_k$ are not on the same side of the line. Thus $\mathbf{x}_k$ is inside the triangle T_h if and only if $N_1(\mathbf{x}_k) > 0$, $N_2(\mathbf{x}_k) > 0$, and $N_3(\mathbf{x}_k) > 0$. When this test fails, our best guess is then to try the triangle on the side corresponding to the most negative weight. Searching elements successively in this manner usually locates the particle in a few steps. This is especially so for a particle code in which, for the sake of accuracy, the particles are not allowed to travel much

more than one zone per time step. In such cases all the particles are found in about three passes. Although we have described the tracking algorithm in terms of triangles, the same technique can be applied to quads in 2D and to tetrahedra and hexadedra (brick elements) in 3D using the appropriate linear functions. A word of caution is in order, however. It is possible, near very irregular concave boundaries, for this method to fail. In this case it would repeatedly point to a location outside the grid as the next guess [R. Löhner, private communication]. However, there are more conservative (and more costly) searching algorithms that can easily be employed as a fallback to make the overall method robust.

5.2. *Charge and Current Assignment*

In this section we describe the charge and current deposition prescriptions that will yield source terms for the Darwin electromagnetic fields. In the continuum, the number, charge, and current densities are linked to the distribution function f_s of a charged particle species s by

$$n(\mathbf{x}, t) = \sum_s \int_\Omega f_s(\mathbf{x}, \mathbf{v}, t)\, d\mathbf{v}$$

$$\rho(\mathbf{x}, t) = \sum_s q_s \int_\Omega f_s(\mathbf{x}, \mathbf{v}, t)\, d\mathbf{v}$$

$$\mathbf{J}(\mathbf{x}, t) = \sum_s q_s \int_\Omega f_s(\mathbf{x}, \mathbf{v}, t)\mathbf{v}\, d\mathbf{v},$$

where the sum on k is taken over all species and q_s is the charge.

In PIC simulations, these functions are approximated by apportioning discrete particle charges and currents to the grid using particle shape functions. These are often taken to be the same as the basis or shape functions on the grid (see Birdsall and Langdon [2]). In our case we will weight the particles to the triangle vertices using the linear basis functions for triangular elements N^i,

$$\rho^i(t) = \frac{1}{V_i}\int_\Omega \rho(\mathbf{x}, t)N^i(\mathbf{x})\, d\mathbf{x}$$

$$= \frac{1}{V_i}\sum_k q_k N^i(\mathbf{x}(t)) \tag{6.2}$$

$$\mathbf{J}^i(t) = \frac{1}{V_i}\int_\Omega \mathbf{J}(\mathbf{x}, t)N^i(\mathbf{x})\, d\mathbf{x}$$

$$= \frac{1}{V_i}\sum_k q_k \mathbf{v}_k N^i(\mathbf{x}(t)) \tag{6.3}$$

where V_i is the volume associated to the node i, i.e., $V_i = \int_\Omega$

now, we simply follow Nielson and Lewis [17] and take the time derivative of the discrete quantities:

$$\frac{d\mathbf{J}^i}{dt} = \frac{1}{V_i}\sum_k q_k \left(\frac{d\mathbf{v}_k}{dt}N^i(\mathbf{x}_k) + \mathbf{v}_k\left(\frac{d\mathbf{x}_k}{dt}\cdot\nabla N^i(\mathbf{x}_k)\right)\right). \tag{6.4}$$

We then substitute

$$\frac{d\mathbf{v}_k}{dt} = \frac{q_k}{m}(\mathbf{E} + \mathbf{v}_k \times \mathbf{B})$$

and

$$\frac{d\mathbf{x}_k}{dt} = \mathbf{v}_k$$

to obtain

$$\frac{d\mathbf{J}^i}{dt} = \frac{1}{V_i}\sum_k q_k \left(\frac{q_k}{m}(\mathbf{E} + \mathbf{v}_k \times \mathbf{B})N^i(\mathbf{x}_k) + \mathbf{v}_k(\mathbf{v}_k\cdot\nabla N^i(\mathbf{x}_k))\right).$$

This expression, which is a source for $\mathbf{E}_{\text{sol}}$, also contains $\mathbf{E}_{\text{sol}}$ in the term involving $\mathbf{E}$. Thus we will take this term over to the left to become part of the elliptic operator.

We now write down the complete time advance algorithm: Starting with $\mathbf{x}^n$, $\mathbf{v}^{n-1/2}$, $\mathbf{E}^n$, and $\mathbf{B}^n$, the particle push yields $\mathbf{v}^{n-1/2}$ and $\mathbf{x}^{n+1}$. Strictly speaking we need $\mathbf{J}^{n+1}$, which, as (6.3) shows, makes use of $\mathbf{v}^{n+1}$ and $\mathbf{x}^{n+1}$. Therefore an extrapolation of the velocity is necessary. We have tried three different ways of time-centering the current source:

- Use the lagged velocities: $\mathbf{v}^{n+1} = \mathbf{v}^{n-1/2}$
- A linear projection: $\mathbf{v}^{n+1} = \frac{3}{2}\mathbf{v}^{n+1/2} - \frac{1}{2}\mathbf{v}^{n-1/2}$
- Do another Boris push using the same fields.

Even though the third method looks like the most accurate one, we have not seen any sensitivities in the results to our choice of time-centering methods. This may come from the fact that $\mathbf{v}^{n+1}$ is just used to predict $\mathbf{J}^{n+1}$, but is not used to advance the particle velocities. At any rate, once $\mathbf{v}^{n+1}$ is computed using any of the above methods, everything we need to compute the sources ρ^{n+1}, $\mathbf{J}^{n+1}$, and $\dot{\mathbf{J}}^{n+1}$ is available. Finally, ϕ^{n+1}, $\mathbf{B}^{n+1}$, and $\mathbf{E}_{\text{sol}}^{n+1}$ are computed using these source terms.

6. NUMERICAL RESULTS

6.1. *The Time Differencing Instability*

The Darwin model for electromagnetic simulation has had a reputation in the literature for being ill-behaved. We suspect

to choose badly. Several authors, including Nielson and Lewis, have noted that violent instabilities can develop from innocent choices for the time-marching scheme. The method we have chosen follows the traditional strategy for solving the Darwin system. Here we take a closer look at the stability problem and conclude that it is the only robust choice. We will focus on the equation involving $\mathbf{E}_{\text{sol}}$:

$$\nabla \times \nabla \times \mathbf{E}_{\text{sol}} - \frac{1}{c^2}\nabla\ddot{\phi} = -\mu_0\dot{\mathbf{J}}.$$

The source term is $\dot{\mathbf{J}}$. The question is whether it is possible to use backward time differencing involving the last two values of $\mathbf{J}$ to obtain $\dot{\mathbf{J}}$. Or even better, could we use Faraday's law and write

$$\nabla \times \mathbf{E}_{\text{sol}}^{n+1} = -\frac{\mathbf{B}^{n+1} - \mathbf{B}^n}{\Delta t} \tag{6.1}$$

and use $\mathbf{B}^n$ and $\mathbf{B}^{n+1}$ which would have already been computed and therefore known? This last scheme would have the considerable advantage of having a solenoidal right-hand side, which would in turn dramatically reduce the number of iterations needed to converge to a solution. Thus, we would like to investigate under what conditions this proposed scheme would be stable. A cold plasma analysis of our scheme similar to what was done by Nielson and Lewis [17] yields the following condition for stability:

$$\frac{\omega_{pe}^2}{c^2k^2} \leq 1.$$

We have explored other explicit schemes and found they yield similar conditions differing by a multiplicative constant of order one. Thus, we take as our stability condition $k \geq \omega_{pe}/c$. Now the smallest k seen by a mesh is π/L, where L is the length of the computational domain. Practically speaking, this means that if $c/\omega_{pe} \geq L/\pi$ the simulation should be stable. Therefore the straightforward time-differencing can be used only for problems of length at most of the order of the collisionless skin depth. But, as the Darwin dispersion analysis (see Appendix A) shows, most interesting Darwin problems lie in a regime where the problem length is several times the collisionless skin depth. Thus abandoning simple time-differencing strategies is unavoidable for most problems and one must determine the source term for $\mathbf{E}_{\text{sol}}$ in other ways. However, let us point out again that there is a stable regime as the following test shows us.

In order to verify the stability constraint discussed above, we have performed the following experiment:

The mesh we used is a square 1m in length with 648 elements of equal size. Numerically $\omega_{pe} \cong 57\sqrt{n}$ and $L = 1\text{m}$. So the algorithm should be stable for $n \leq 2.7 \times 10^{14}\text{m}^{-3}$. We used a time step of 10^{-13}s so that $\omega_{pe}\Delta t < 2$ was satisfied for all the densities we used. We loaded 6400 electrons uniformly on the grid, and an equal charge of opposite sign was added to represent the ions, so that the plasma was neutral. To generate a perturbation we set the electrons drifting at 1m/s. Thus there was essentially no electrostatic field, but rather a small perturbed magnetic field and a small solenoidal electric field.

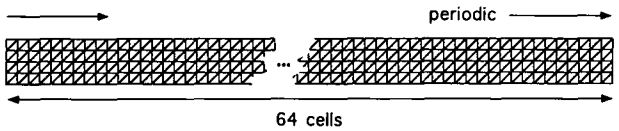

FIG. 4. The triangulation for the periodic test cases used in evaluating the dispersion relations.

Several densities were used ranging from 10^{12} to 10^{18}m^{-3}. Up to $10^{14}\ m^{-3}$ the simulation remained stable, generating a small, but stable solenoidal electric field which remained so over the 300 time steps of the computation. At a density of 10^{15}m^{-3}, the electric field as well as the magnetic field began to increase dramatically, showing a very violent instability and destroying the simulation after fewer than 10 time steps. The same phenomenon was observed for higher densities, with the blowup coming even earlier. We noted that decreasing the time step did not help, confirming that the stability is independent of time step in this regime.

6.2. *Numerical Tests of the Dispersion Relation in a Doubly Periodic Domain*

To validate the code without introducing the additional complexity of boundary conditions, we consider a doubly periodic 2D computational domain (see Fig. 4).

A few electrostatic runs were performed to confirm that the code yielded the correct frequencies for both cold and warm plasma oscillations. Energy conservation was very good, as well—better than 3% over 16,000 time steps for $\omega_{pe}\Delta t \approx 0.3$.

To validate the Darwin field solver, we attempted to reproduce numerically the dispersion relations we computed analytically in Appendix A for a cold plasma. The parameters for these runs were as follows: The fine grid consisted of 4×64 squares of length 1mm on a side divided into two right triangles. Thus the computational domain was 4mm wide and 64 mm long. We also had

$$n_i = n_e = 10^{18}\text{m}^{-3}$$

$$m_e = 9.1 \times 10^{-31}\,\text{kg}$$

$$m_i = 4m_e$$

$$B_0 = 0.38\ T.$$

We started these runs by superposing four modes and letting the waves propagate. A spatial FFT was used to separate the different modes to obtain a time history. We ran the problem

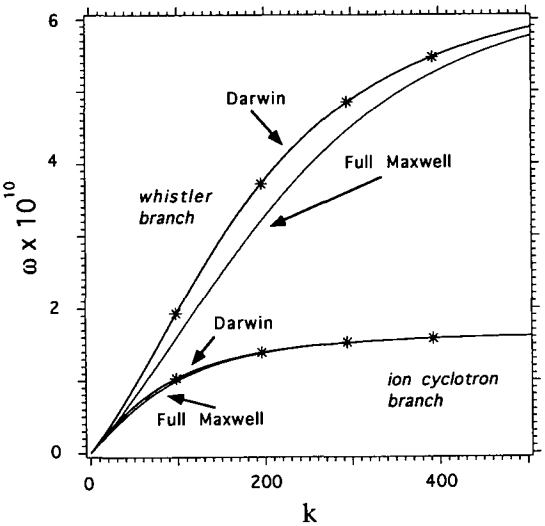

FIG. 5. Dispersion curves for modes propagating perpendicular to the magnetic field direction. The solid lines are analytic results for the full set of Maxwell's equations and for the Darwin approximation. The code results are marked with asterisks.

for 2048 time steps. A FFT on the sampled time series was used to obtain the frequencies associated with each mode. The results shown in Figs. 5 and 6, were very good. The points lie almost exactly on the analytical curves corresponding to the Darwin equations.

6.3. *Numerical Tests Involving a Bounded Domain*

In order to exercise the axisymmetric version of our code and to test its robustness in complex bounded geometries we designed a hypothetical Darwin problem as follows:

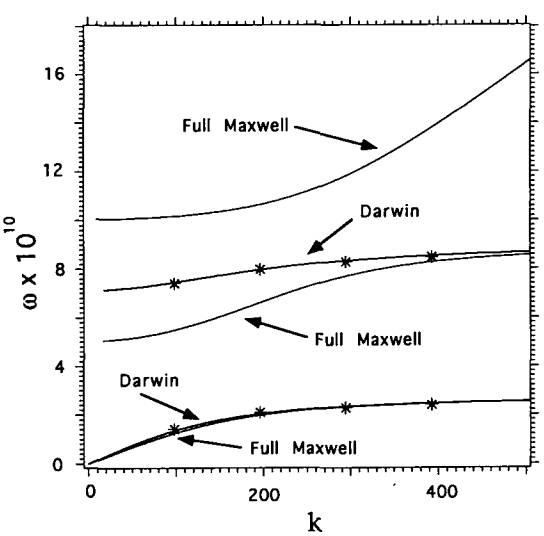

FIG. 6. Dispersion curves for modes propagating parallel to the magnetic field.

The geometry of our device was chosen to be complex enough to necessitate an unstructured grid. It is reminiscent of a linear accelerator module, although it does not represent any existing one.

In this simulation, a driving voltage $V = V_0(1 + \sin \omega t)$, with $V_0 = 0.5$ kV and $\omega = 4\ 10^9 s^{-1}$ was applied to the conducting boundaries. Electrons were injected with an energy of 10 eV, and a constant axial magnetic field $B_0 = 0.5\ T$ (=5 kG) was applied to avoid an expansion of the beam.

In order to make the Darwin model more interesting, we sought a regime where $\delta x/c \ll \delta x/v$, thus making the usual electromagnetic time steps, restricted by the Courant condition, costly.

We chose $\Delta t = 2.5 \times 10^{-10}$ s so that a particle could not travel much more than one grid cell per time step. There is no way in a PIC code to overcome this limitation if physically meaningful results are to be expected. We ran the code over 500 time steps, corresponding to many device transit times for the particles. During the run, we encountered no stability problems and obtained reasonable results (plausible field magnitudes, currents, etc.) for fields and sources. A snaphot of the simulation is shown in Figs. 7 and 8.

7. CONCLUSION

The code we have developed is based on solid mathematics and the accumulated experience of many investigators who have explored this somewhat arcane variant on Maxwell's equations. We have attempted in this paper to synthesize several developments in the art of PIC simulation as applied to moderate-to-long time scale electromagnetic phenomena. We have formulated a PIC method based on the Darwin approximation that can be used on unstructured meshes. This removes many geometrical limitations and allows access to a host of problem domains related to real plasma devices. In doing so, we have also incorporated recent work in the mathematical foundations of the Darwin approximation, especially as it affects the choice of well-posed boundary conditions. Furthermore, the variational formulation applied here may be shown to be a good alternative to the streamlined methods introduced by Hewett *et al.* [4, 11] to make implementations of the Darwin schemes more affordable (see Appendix C).

We have attempted to nail down, by means of the dispersion relations and dimensional analysis, the regime in which the Darwin approximation is likely to be most useful. This is something which current practitioners have admitted is sometimes bewildering. We have benchmarked the code against a dispersion analysis to show that the variational formulation is indeed correct and accurate. Finally, we presented a simple test problem to show that the code was well-behaved in a complex geometry with both metallic and open boundaries.

We believe that the Darwin approximation has a place in the repertoire of plasma simulation because it represents a form of the full system that is reduced only by the loss of propagating

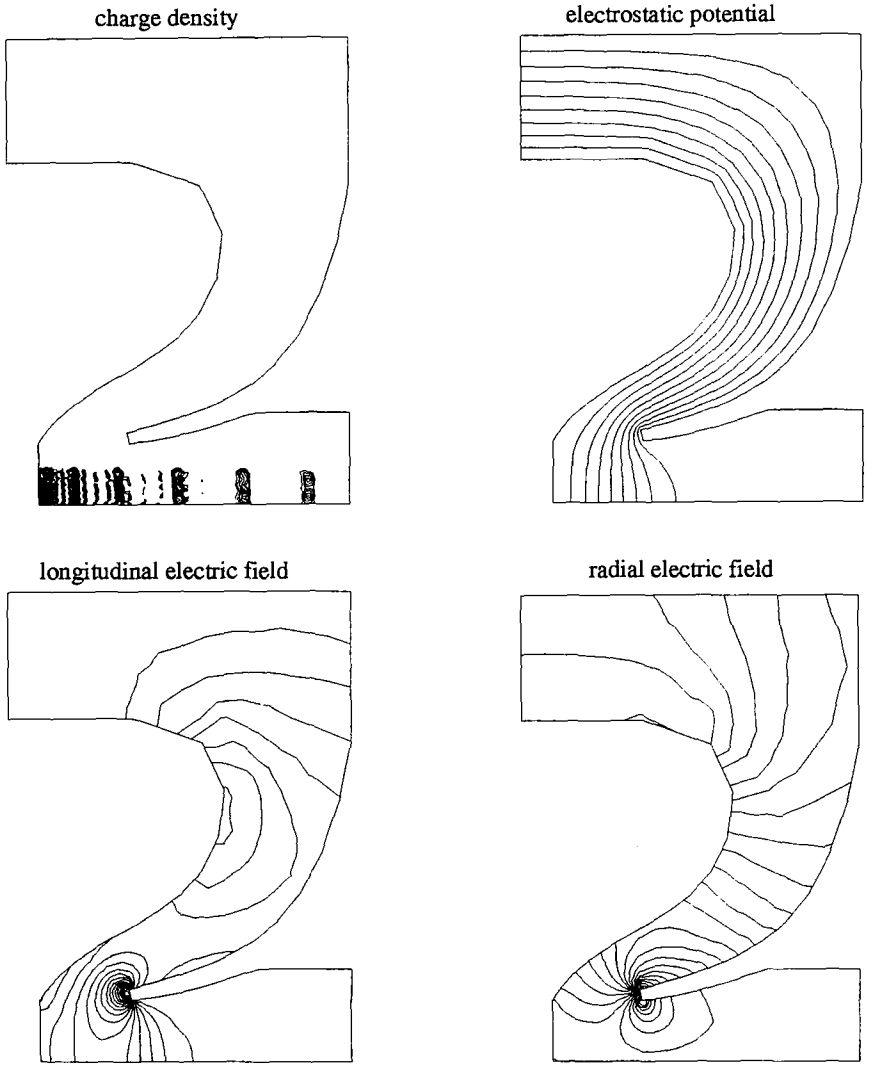

FIG. 7. The results of a bounded problem involving a hypothetical device reminiscent of an accelerator geometry. Clockwise, snapshots of the charge density, the electrostatic potential, the radial electric field and the longitudinal electric field.

electromagnetic waves. Unlike implicit formulations, with their time step-dependent dispersion relations, the Darwin method is a clean representation of the Vlasov–Maxwell system in a low frequency regime that can be readily analyzed and understood. However, there are always limitations. In particular, eliminating the Courant condition on the field solution does not help stiffness associated with the plasma frequency. Nevertheless, there are straightforward electrostatic particle-implicit techniques that may be applied to alleviate this problem.

Finally, we think this paper is valuable for another reason in that it is a good example of recent mixed-variational techniques applied to problems with local vector–field constraints. These methods are very powerful in their ability to bring finite element methods and, therefore, geometric flexibility into areas where they would not have been applied in the past. We have seen them applied to the full Maxwell equations with the work of Assous *et al.* [1] and to the Darwin formulation here. We also expect them to be useful in MHD and in quasineutral hybrid formulations. Thus the whole field of plasma simulation could be opened to unstructured meshes allowing much greater flexibility in simulating real plasma devices.

APPENDIX A: DISPERSION ANALYSIS OF THE DARWIN FIELD EQUATIONS

In order to gain insight into the problem regime appropriate to the Darwin model, we performed a dispersion analysis comparing the full electromagnetic equations, the Darwin equations, and the quasistatic equations.

A dispersion relation can be computed for each of the different models. For simplicity, we have used the linearized fluid equations to represent the particles (e.g., see Stix [20]). Let

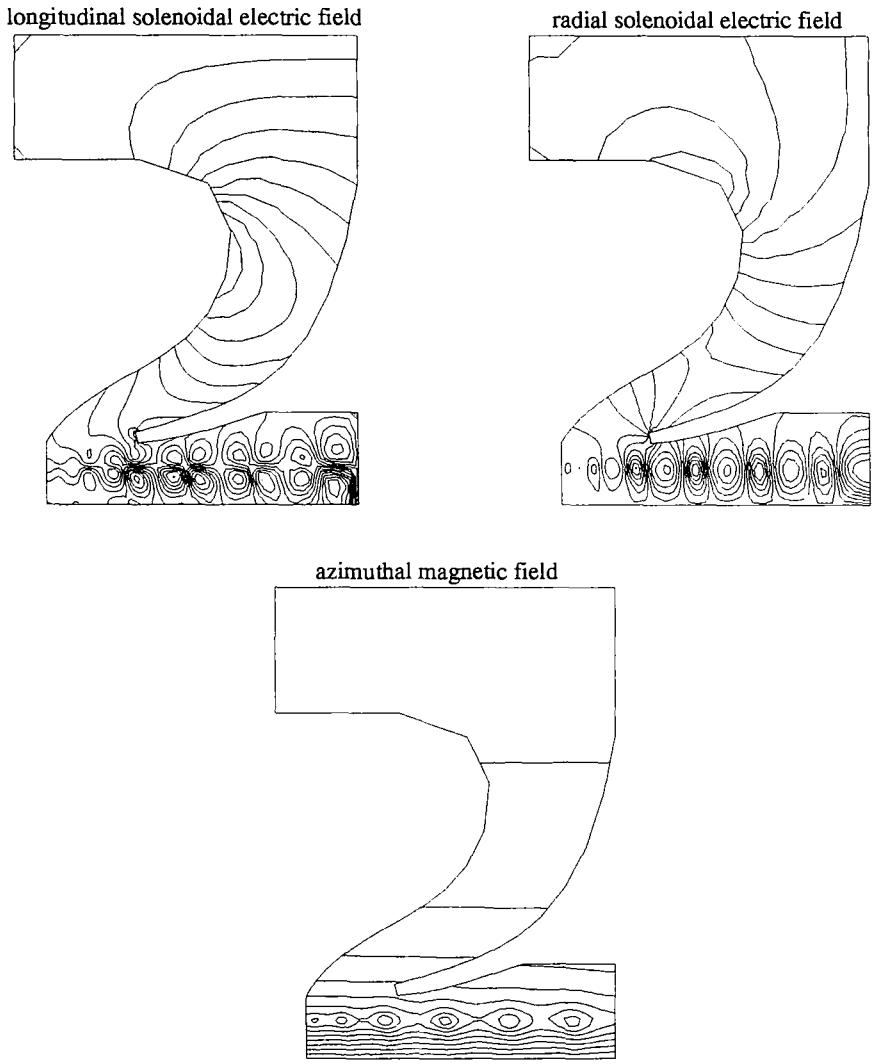

FIG. 8. The results of a bounded problem involving a hypothetical device reminiscent of an accelerator geometry. Clockwise, snapshots of the longitudinal solenoidal electric field, the radial solenoidal electric field and the azimuthal magnetic field.

$n = ck/\omega$ be the refractive index. We introduce the following definitions:

$$\alpha = \frac{1}{\omega^2}\left(\frac{\omega_{pi}^2}{1-\omega_{ci}^2/\omega^2} + \frac{\omega_{pe}^2}{1-\omega_{ce}^2/\omega^2}\right)$$

$$\beta = \frac{1}{\omega^2}\left(\frac{\omega_{ci}}{\omega}\frac{\omega_{pi}^2}{1-\omega_{ci}^2/\omega^2} + \frac{\omega_{ce}}{\omega}\frac{\omega_{pe}^2}{1-\omega_{ce}^2/\omega^2}\right)$$

$$\gamma = \frac{1}{\omega^2}(\omega_{pi}^2 + \omega_{pe}^2).$$

These appear in the expression for the dielectric tensor. Physically β is a dielectric constant, while α and γ are susceptibilities. Without loss of generality we suppose that we have a constant $\mathbf{B}_0$ along the axis $\hat{z}$ and that the wave vector $\mathbf{k} = k \sin\theta\,\hat{x} + k\cos\theta\,\hat{z}$. The monochromatic waves are assumed to be of the form $e^{i(k\cdot x-\omega t)}$.

The dispersion relations may be written as follows:

- For the full Maxwell equations,

$$\tan^2\theta = \frac{-(1-\gamma)(n^2-1+\alpha+\beta)(n^2-1+\alpha-\beta)}{(n^2-(1-\gamma))((1-\alpha)n^2-((1-\alpha)^2-\beta^2))};$$

- For the Darwin equations,

$$\tan^2\theta = \frac{-(1-\gamma)(n^2+\alpha+\beta)(n^2+\alpha-\beta)}{(n^2+\gamma)((1-\alpha)n^2-\alpha^2+\beta^2+\alpha)};$$

- For the quasistatic equations (i.e., static electric and magnetic fields) we merely have

$$\tan^2\theta = \frac{-(1-\gamma)}{1-\alpha}.$$

We now compare these dispersion relations in a few special cases. Consider $\mathbf{B}\|\mathbf{k}$ (i.e., $\theta = 0$).

• Plasma oscillations. This corresponds to $\gamma = 1$ in the dispersion relation, that is,

$$\omega^2 = \omega_{pi}^2 + \omega_{pe}^2.$$

All three field equations (full Maxwell, Darwin, and electrostatic) support this wave exactly.

• The R wave. In the Maxwell dispersion relation this corresponds to $n^2 = 1 - (\alpha - \beta)$, that is,

$$n^2 = 1 - \frac{\omega_{pe}^2 + \omega_{pi}^2}{(\omega - \omega_{ce})(\omega + \omega_{ci})},$$

provided the ions have only one positive charge, which we will assume, as well as $n_i = n_e$, $\omega_{pi} \ll \omega_{pe}$ and $\omega_{ci} \ll \omega_{ce}$.

The corresponding wave in the Darwin approximation is $n^2 = -(\alpha - \beta)$, that is,

$$n^2 = -\frac{\omega_{pe}^2 + \omega_{pi}^2}{(\omega - \omega_{ce})(\omega + \omega_{ci})}.$$

Since this wave is transverse electromagnetic it does not exist in the quasistatic approximation.

Let $v_A = \mathbf{B}/\sqrt{\rho\mu_0}$ be the Alfven velocity, where $\rho = m_i n_i$ is the mass density of the ions. In both the Darwin and the full Maxwell cases, the refractive index $n^2(\omega)$ has a minimum at $\omega = \omega_{ce}/2$. This minimum value is $n^2 = 1 + 4(\omega_{pe}^2/\omega_{ce}^2)$ for Maxwell and $n^2 = 4(\omega_{pe}^2/\omega_{ce}^2)$ for Darwin. If $\omega_{pe} \gg \omega_{ce}$ (high density plasma or low $\mathbf{B}$), this minimum is approximately the same for Darwin and Maxwell. This is not true for $\omega_{pe} \ll \omega_{ce}$.

What one finds from this comparison is that in the limit $\omega_{pe} \gg \omega_{ce}$ (whistler waves) the Darwin approximation is very good at all frequencies less than ω_{ce}. The entire low frequency branch is given with perfect accuracy by the Darwin approximation. However, when $\omega_{pe} \ll \omega_{ce}$ Darwin is a good approximation only for $\omega \ll \omega_{ce}$ and for ω close to ω_{ce}.

The high frequency branch of the R wave is completely damped out in the Darwin approximation.

• The L wave. In the Maxwell dispersion relation this corresponds to $n^2 = 1 - (\alpha + \beta)$, that is,

$$n^2 = 1 - \frac{\omega_{pe}^2 + \omega_{pi}^2}{(\omega + \omega_{ce})(\omega - \omega_{ci})}.$$

The corresponding wave in the Darwin approximation is $n^2 = -(\alpha + \beta)$, that is,

$$n^2 = -\frac{\omega_{pe}^2 + \omega_{pi}^2}{(\omega + \omega_{ce})(\omega - \omega_{ci})}.$$

This wave is transverse electromagnetic and does not exist in the quasistatic approximation.

For the L wave, the Darwin approximation recovers the low frequency branch ($\omega < \omega_{ci}$) very well in the limit as $c^2/V_a^2 \gg 1$. Again the high frequency branch does not exist.

At very low frequencies ($\omega \ll \omega_{ci}$) the ion cyclotron and electron cyclotron wave come together in one branch satisfying

$$n^2 = \frac{\omega_{pi}^2}{\omega_{ci}^2} = \frac{c^2}{v_A^2}$$

both for Maxwell and Darwin, assuming that $c^2/v_A^2 \gg 1$, which is normally the case. This can also be written

$$\omega^2 = k^2 v_A^2$$

which we recognize as the dispersion relation for Alfven waves.

Next consider $\mathbf{B}\perp\mathbf{k}$ (i.e., $\theta = \pi/2$).

• The ordinary wave. The index of refraction for the full Maxwell equations is obtained by setting $n^2 = 1 - \gamma$, i.e.,

$$n^2 = 1 - \frac{\omega_{pe}^2}{\omega^2}.$$

The same wave in the Darwin approximation is described by $n^2 = -\gamma$, that is,

$$n^2 = -\frac{\omega_{pe}^2}{\omega^2}.$$

This wave is not present in the quasistatic approximation.

We note that n^2 is always negative for Darwin, meaning that the wave is always damped out. Thus the ordinary wave does not exist in the Darwin approximation.

• The extraordinary wave. The Maxwell equation limit corresponds to $(1 - \alpha)n^2 - ((1 - \alpha)^2 - \beta^2) = 0$, that is,

$$n^2 = 1 - \frac{(\omega_{pe}^2 + \omega_{pi}^2)(\omega^2 - \omega_{pe}^2 - \omega_{pi}^2 - \omega_{ce}\omega_{ci})}{(\omega^2 - \omega_{ce}^2)(\omega^2 - \omega_{ci}^2) - (\omega_{pe}^2 + \omega_{pi}^2)(\omega^2 - \omega_{ce}\omega_{ci})}.$$

In the Darwin approximation we have $(1 - \alpha)n^2 - \alpha^2 + \beta^2 + \alpha = 0$, that is,

$$n^2 = \frac{(\omega_{pe}^2 + \omega_{pi}^2)(\omega^2 - \omega_{pe}^2 - \omega_{pi}^2 - \omega_{ce}\omega_{ci})}{(\omega^2 - \omega_{ce}^2)(\omega^2 - \omega_{ci}^2) - (\omega_{pe}^2 + \omega_{pi}^2)(\omega^2 - \omega_{ce}\omega_{ci})}.$$

We also have something in the quasistatic approximation, $1 - \alpha = 0$, that is,

$$\omega^2 = \frac{\omega_{pi}^2}{1 - \omega_{ci}^2/\omega^2} + \frac{\omega_{pe}^2}{1 - \omega_{ce}^2/\omega^2}.$$

At high frequencies this corresponds to plasma oscillations, but at low frequencies $\omega^2 < 0$, so it is damped away.

We shall now take a closer look at the extraordinary wave in the full Maxwell equations and in the Darwin case. We note that a resonance is obtained for $n^2 \to +\infty$.

Looking at the dispersion relations, we see that Maxwell and Darwin have the same resonance frequencies, which are the roots of

$$(\omega^2 - \omega_{ce}^2)(\omega^2 - \omega_{ci}^2) - (\omega_{pe}^2 + \omega_{pi}^2)(\omega^2 - \omega_{ce}\omega_{ci}) = 0.$$

Keeping in mind that $\omega_{ci} \ll \omega_{ce}$ and $\omega_{pi} \ll \omega_{pe}$, and neglecting terms according, the equations can be written

$$\omega^4 - (\omega_{ce}^2 + \omega_{ci}^2 + \omega_{pe}^2 + \omega_{pi}^2)\omega^2 + \omega_{ce}\omega_{ci}(\omega_{pe}^2 + \omega_{pi}^2 + \omega_{ce}\omega_{ci}) = 0.$$

Let $\omega_h^2 = \omega_{ce}^2 + \omega_{ci}^2 + \omega_{pe}^2 + \omega_{pi}^2$. We have

$$\omega^2 = \tfrac{1}{2}(\omega_h^2 \pm (\omega_h^4 - 4\omega_{ce}\omega_{ci}(\omega_{pe}^2 + \omega_{pi}^2 + \omega_{ce}\omega_{ci}))^{1/2}),$$

but $\omega_h \geq \omega_{ce} \gg \omega_{ci}$, so

$$\omega^2 = \frac{1}{2}\left(\omega_h^2 \pm \left(\omega_h^2 - 2\omega_{ce}\omega_{ci}\left(\frac{\omega_{pe}^2 + \omega_{ce}\omega_{ci}}{\omega_h^2}\right)\right)\right).$$

Thus, we get two resonant frequencies

$$\omega_{\mathrm{H}} = \left(\omega_h^2 - \omega_{ce}\omega_{ci}\left(\frac{\omega_{pe}^2 + \omega_{ce}\omega_{ci}}{\omega_h^2}\right)\right)$$

and

$$\omega_{\mathrm{LH}} = \sqrt{\omega_{ce}\omega_{ci}}\left(\frac{\omega_{pe}^2 + \omega_{ce}\omega_{ci}}{\omega_h^2}\right);$$

ω_{H} is recognized as the upper hybrid frequency and is actually very close to ω_h, and ω_{LH} is the lower hybrid frequency.

We also note a cutoff occurs when $n^2 = 0$. For the Darwin model this happens when

$$\omega^2 = \omega_{pe}^2 + \omega_{pi}^2 + \omega_{ci}\omega_{ce} \approx \omega_{pe}^2 + \omega_{ci}\omega_{ce}.$$

Call this value ω_{ID}. For the full Maxwell case cutoff occurs when

$$(\omega^2 - \omega_{ce}^2)(\omega^2 - \omega_{ci}^2) - (\omega_{pe}^2 + \omega_{pi}^2)(\omega^2 - \omega_{ce}\omega_{ci}) = (\omega_{pe}^2 + \omega_{pi}^2)(\omega^2 - \omega_{pe}^2 - \omega_{pi}^2 - \omega_{ce}\omega_{ci}),$$

with the usual approximations, this becomes

$$\omega^2 = \frac{\omega_{ce}^2}{2}\left(1 + 2\frac{\omega_{pe}^2}{\omega_{ce}^2} \pm \left(1 + 4\frac{\omega_{pe}^2}{\omega_{ce}^2}\right)^{1/2}\right).$$

So for the Maxwell limit we have two cutoff frequencies, namely,

$$\omega_{1M} = \frac{\omega_{ce}}{2}\left(-1 + \left(1 + 4\frac{\omega_{pe}^2}{\omega_{ce}^2}\right)^{1/2}\right)$$

$$\omega_{2M} = \frac{\omega_{ce}}{2}\left(1 + \left(1 + 4\frac{\omega_{pe}^2}{\omega_{ce}^2}\right)^{1/2}\right).$$

Thus, it appears that in this case the Darwin approximation is very good for the whole lower hybrid branch as well as for frequencies close to the upper hybrid frequency. Here again, the high frequency branch is completely damped out.

In summary, the Darwin approximation, as expected, describes all the low frequency electromagnetic phenomena very accurately. However, such phenomena depend on the existence of a strong magnetic field. This suggests that the Darwin approximation is made-to-order for strongly magnetized plasma, where the phenomena of interest are low-frequency electromagnetic plasma waves, particularly those near the lower hybrid branch.

APPENDIX B: FINITE ELEMENT FORMULATIONS FOR (3.11)–(3.12) AND (3.13)–(3.14)

For the discretization of (3.11)–(3.12) and (3.13)–(3.14) we introduce Y_h and M_h defined by

$$Y_h = \{C_h \in C^0(\overline{\Omega})^3;\ \forall T_h \in \tau_h\ C_{h,\mathrm{K}_h} \in P_1^3\}$$

$$M_{2h} = \{q_{2h} \in C^0(\overline{\Omega});\ \forall T_{2h} \in \tau_{2h}\ q_{2h,K_{2h}} \in P_1\}.$$

For any $C_h \in Y_h$ we may write

$$C_h(\mathbf{x}) = \sum_{\alpha=1}^{3}\sum_{i=1}^{n_h} C_\alpha^i N^i(\mathbf{x})\mathbf{u}_\alpha,$$

where $(\mathbf{u}_1, \mathbf{u}_2, \mathbf{u}_3)$ are the three-dimensional basis vectors in $\mathbb{R}^3$. The set $(N^i\mathbf{u}_\alpha)_{1\leq i\leq n_h, 1\leq\alpha\leq 3}$ is a basis of Y_h.

For any $q_{2h} \in M_{2h}$ we may write

$$q_{2h} = \sum_{i=1}^{n_{2h}} q^i M^i(\mathbf{x}),$$

where $(M^i)_{1\le i\le n_{2h}}$ is a basis of M_{2h}. The set $(M^i)_{1\le i\le n_{2h}}$ is defined on τ_{2h} in the same way that $(N^i)_{1\le i\le n_h}$ is defined on τ_h.

We prefer not to put the essential boundary conditions $\mathbf{B}\cdot n = 0$ or $\mathbf{E}\times\mathbf{n} = 0$ in the finite dimensional spaces but to use a projected conjugate gradient, as described in [16] to enforce them. A detailed discussion is given in Assous *et al.* [1].

We now write down our finite element formulation of (3.11)–(3.12) and (3.13)–(3.14). The derivations are straightforward and are analogous to the one for the electrostatic potential.

$B_h(\mathbf{x}, t) = \sum_{\alpha=1}^{3}\sum_{i=1}^{n_h} B_\alpha^i(t)N^i(\mathbf{x})\mathbf{u}_\alpha$ and $p_{2h}(\mathbf{x}, t) = \sum_{i=1}^{n_{2h}} p^i(t)M^i(\mathbf{x})$ are solutions of

$$\sum_{\alpha=1}^{3}\sum_{i=1}^{n_h}\left(B_\alpha^i\left(\int_\Omega \nabla\times(N^i\mathbf{u}_\alpha)\cdot\nabla\times(N^j\mathbf{u}_\beta)\,d\mathbf{x} + \int_\Omega \nabla\cdot(N^i\mathbf{u}_\alpha)\,\nabla\cdot(N^j\mathbf{u}_\beta)\,d\mathbf{x}\right) + \frac{1}{c}\frac{d\mathbf{B}_\alpha^i}{dt}\int_{\Gamma_2}(N^i\mathbf{u}_\alpha\times n)\cdot(N^j\mathbf{u}_\beta\times n)\,d\sigma\right) + \sum_{i=1}^{n_{2h}} p^i\int_\Omega M^i\nabla\cdot(N^j\mathbf{u}_\beta)\,d\mathbf{x} = \mu_0\sum_{\alpha=1}^{3}\sum_{i=1}^{n_h} J_\alpha^i\int_\Omega (N^i\mathbf{u}_\alpha)\cdot\nabla\times(N^j\mathbf{u}_\beta)\,d\mathbf{x}$$

for $1\le j\le n_h$, $1\le\beta\le 3$,

$$\sum_{\alpha=1}^{3}\sum_{i=1}^{n_h} B_\alpha^i\int_\Omega \nabla\cdot(N^i\mathbf{u}_\alpha)\cdot M^j\,d\mathbf{x} = 0$$

for $1\le j\le n_{2h}$.

$E_{\mathrm{sol}\,h}(\mathbf{x}, t) = \sum_{\alpha=1}^{3}\sum_{i=1}^{n_h} E_{\mathrm{sol}\,\alpha}^i(t)N^i(\mathbf{x})\mathbf{u}_\alpha$ and $\ddot{\phi}_{2h}(\mathbf{x}, t) = \sum_{i=1}^{n_{2h}}\ddot{\phi}^i(t)M^i(\mathbf{x})$ are solutions of

$$\sum_{\alpha=1}^{3}\sum_{i=1}^{n_h} E_{\mathrm{sol}\,\alpha}^i\left(\int_\Omega \nabla\times(N^i\mathbf{u}_\alpha)\cdot\nabla\times(N^j\mathbf{u}_\beta)\,d\mathbf{x} + \int_\Omega \nabla\cdot(N^i\mathbf{u}_\alpha)\,\nabla\cdot(N^j\mathbf{u}_\beta)\,d\mathbf{x}\right) + \frac{1}{c^2}\sum_{i=1}^{n_{2h}}\ddot{\phi}^i\int_\Omega M^i\nabla\cdot(N^j\mathbf{u}_\beta)\,d\mathbf{x} = -\mu_0\sum_{\alpha=1}^{3}\sum_{i=1}^{n_h}\dot{J}_\alpha^i\int_\Omega (N^i\mathbf{u}_\alpha)\cdot(N^j\mathbf{u}_\beta)\,d\mathbf{x} + \frac{1}{c^2}\sum_{i=1}^{n_{2h}}\ddot{V}^i\int_{\Gamma_1} M^iN^j\mathbf{u}_\beta\cdot\mathbf{n}\,d\sigma - \frac{1}{c}\sum_{\alpha=1}^{3}\sum_{i=1}^{n_h}\frac{dE_{\mathrm{int}\,\alpha}^i}{dt}\int_{\Gamma_2} N^iN^j(\mathbf{u}_\alpha\times\mathbf{n})\cdot(\mathbf{u}_\beta\times\mathbf{n})\,d\sigma$$

for $1\le j\le n_h$, $1\le\beta\le 3$,

$$\sum_{\alpha=1}^{3}\sum_{i=1}^{n_h} E_{\mathrm{sol}\,\alpha}^i\int_\Omega \nabla\cdot(N^i\mathbf{u}_\alpha)\cdot M^j\,d\mathbf{x} = 0 \quad \text{for } 1\le j\le n_{2h}.$$

APPENDIX C: MIXED FORMULATION VS STREAMLINED DARWIN

As we have seen $\mathbf{E}_{\mathrm{sol}}$ is solution of the system

$$\nabla\times\nabla\times\mathbf{E}_{\mathrm{sol}} - \nabla\ddot{\phi} = -\dot{J}$$
$$\nabla\cdot\mathbf{E}_{\mathrm{sol}} = 0.$$

Having adequate boundary conditions, say for example $\mathbf{E}_{\mathrm{sol}}\times\mathbf{n} = 0$ and $\ddot{\phi} = 0$ if the boundary is perfectly conducting, the variational theory enables us to show that there is a unique solution $(\mathbf{E}_{\mathrm{sol}}, \ddot{\phi})$, $\ddot{\phi}$ being a by-product we do not actually compute. In this paper we describe a method allowing us to work directly on this formulation which we call a mixed formulation. Let us compare this method to the streamlined Darwin algorithm introduced by Hewett and Boyd [4] which reads: Compute the $\mathbf{F}$ and ψ solution of

$$\nabla^2\mathbf{F} = \dot{\mathbf{J}}$$
$$\nabla^2\psi = \nabla\cdot\mathbf{F}$$

and then $\mathbf{E}_{\mathrm{sol}} = \mathbf{F} - \nabla\psi$. $\mathbf{E}_{\mathrm{sol}}$ computed this way is identical to the first one; indeed,

$$\nabla\times\nabla\times\mathbf{E}_{\mathrm{sol}} = \nabla\times\nabla\times\mathbf{F} = -\nabla^2\mathbf{F} + \nabla\nabla\cdot\mathbf{F}.$$

Hence

$$\nabla\times\nabla\times\mathbf{E}_{\mathrm{sol}} - \nabla(\nabla^2\psi) = -\dot{\mathbf{J}}$$
$$\nabla\cdot\mathbf{E}_{\mathrm{sol}} = 0$$

and, thus, the variational theory tells us that the unique solution to this system—with the same boundary conditions as previously—is $(\mathbf{E}_{\mathrm{sol}}, \nabla^2\psi)$. Therefore $\mathbf{E}_{\mathrm{sol}}$ computed with this algorithm is identical to the first one and, additionally, $\nabla^2\psi = \ddot{\phi}$.

The streamlined Darwin formulation seems to have the advantage of having two decoupled equations. However, this is true only when $\dot{\mathbf{J}}$ can be time differenced, which is not the case, as we have seen, in most Darwin applications. As for the boundary conditions, you can pick anything, for example, Dirichlet 0 for ψ, and then the boundary conditions on $\mathbf{F}$ are given by those on $\mathbf{E}_{\mathrm{sol}}$. Hence the boundary conditions issue is identical for both algorithms.

Hewett *et al.* [11] have developed fast ADI-based methods for the streamlined formulation. These cannot be applied on unstructured meshes. However, the mixed formulation using different functional spaces for the fields and the Lagrange multi-

pliers lead to slightly smaller problems. Moreover, $\mathbf{E}_{sol}$ is obtained directly without having to take the gradient of a scalar potential which gives greater accuracy.

ACKNOWLEDGMENTS

The authors thank Pierre Degond and Dennis Hewett for many helpful discussions. This work was performed in part under the auspices of the U.S. Department of Energy by Lawrence Livermore National Laboratory under Contract W-7405-Eng-48.

REFERENCES

1. F. Assous, P. Degond, E. Heintze, P.-A. Raviart, and J. Segré, *J. Comput. Phys.* **109**(2), 222 (1993).
2. C. K. Birdsall and A. B. Langdon, *Plasma Physics via Computer Simulation* (McGraw–Hill, New York, 1985).
3. J. Busnardo-Neto, P. L. Pritchett, A. T. Lin, and J. M. Dawson, *J. Comput. Phys.* **23,** 300 (1977).
4. D. W. Hewett and J. K. Boyd, *J. Comput. Phys.* **70,** 166 (1986).
5. F. Hermeline, *J. Comput. Phys.* **106,** 1 (1993).
6. D. W. Hewett, Low-frequency electromagnetic (Darwin) applications in plasma simulation, *Comput. Phys. Commun.*, to appear.
7. R. W. Hockney and J. W. Eastwood, *Computer Simulation Using Particles* (McGraw-Hill, New York, 1981).
8. P. Degond and P. A. Raviart, *Forum Math.* **4,** 13 (1992).
9. M. Fortin and R. Glowinski, *Augmented Lagrangian Methods*, Comput. Math., Vol. 5 (Springer-Verlag, New-York/Berlin, 1986).
10. V. Girault and P.-A. Raviart, *Finite Element Methods for Navier–Stokes Equations*, Comput. Math. (Springer-Verlag, New York/Berlin, 1986).
11. D. W. Hewett, D. J. Larson, and S. Doss, *J. Comput. Phys.* **101,** 11 (1992).
12. D. W. Hewett and C. W. Nielson, *J. Comput. Phys.* **29,** 219 (1978).
13. M. E. Jones, "Electromagnetic PIC Codes with Body-Fitted Coordinates," in *12th Conference on the Numerical Simulation of Plasma, San Francisco, CA, Sept. 20–23, 1987.*
14. R. Löhner and J. Ambrosiano, *J. Comput. Phys.* **91,** 22 (1990).
15. N. K. Madsen and R. W. Ziolkowsky, *Electromagnetics* **10,** 147 (1990).
16. B. Métivet, B. Thomas, and P. Fullsack, *Rapport* EDF HI-72/6069 (unpublished).
17. C. W. Nielson and H. R. Lewis, *Methods Comput. Phys.* **16,** 367 (1976).
18. C. Parrot, thesis, University Paris 6, 1993 (unpublished).
19. D. Seldner and T. Westermann, *J. Comput. Phys.* **79,** 1 (1988).
20. T. Stix, *The Theory of Plasma Waves* (McGraw–Hill, New York, 1962).
21. H. Weitzner and W. Lawson, *Phys. Fluids. B* **1,** 1953 (1989).